

Computational Studies of Structures and Dynamics of 1,3-Dimethylimidazolium Salt Liquids and their Interfaces Using Polarizable Potential Models[†]

Tsun-Mei Chang

Department of Chemistry University of Wisconsin—Parkside 900 Wood Road, Box 2000 Kenosha, Wisconsin 53141

Liem X. Dang*

Chemical and Materials Sciences Division Pacific Northwest National Laboratory Richland, Washington 93352

Received: October 15, 2008; Revised Manuscript Received: November 20, 2008

The structures, thermodynamics, and dynamical properties of bulk and air/liquid interfaces of three ionic liquids, 1,3-dimethylimidazolium [dmim]⁺ with Cl⁻, Br⁻, and I⁻ were studied using molecular dynamics techniques and polarizable potential models. In bulk melts, the radial distribution functions reveal a significant long-range structural correlation in these ionic liquids. The single-ion dynamics are studied via mean-square-displacements, velocity and orientational correlation functions. We observe that anion size plays an important role in the dynamics of ionic liquids, with larger anions inducing faster cation and anion motion. The computed density profiles of the ionic liquid/vapor interface exhibit oscillatory behavior, indicative of surface layering at the interface. The computed surface tensions indicate small differences between these ionic liquids and decrease with the increasing anion size. The magnitudes of the computed potential drops of these ionic liquids are found to be small and negative and increase with the decreasing anion size. These results could imply that the cation dipoles on average orient more in the interfacial plane than perpendicular to it. Our results showed that anion type plays a major role in determining IL interfacial behavior.

I. Introduction

Room temperature ionic liquids have attracted significant attention in recent years due to their unusual chemical and physical properties.^{1–5} The term “room temperature ionic liquids” refers to molten salts that are liquids near room temperature and generally consist of large organic cations and inorganic anions. Typically, ionic liquids are nonflammable, have low vapor pressure, high ionic conductivity, and high thermal stability. Because of the broad selection of anion-cation combinations, ionic liquids have great potential to be tailor-made for specific applications and have been widely used in many fields, including synthesis and catalysis,^{3,6,7} electrochemistry,^{8–10} and liquid–liquid extraction.¹¹ Due to their nonvolatile nature, ionic liquids are regarded environmentally friendly “green solvents”, and can be used as designer solvents for a broad range of chemical processes. An understanding of ionic liquids at the molecular level will aid in this direction.

In addition to synthesis and preparation of novel ionic liquids,^{3,12,13} intensive research efforts have contributed to our knowledge of ionic liquids. Experimental techniques including spectroscopy, optical microscopy, calorimetry, and neutron diffraction methods have been employed to study the molecular interactions, structures, and dynamics of bulk ionic liquids. Phase behavior, density, viscosity, conductivity, and transport properties have also been determined.^{14–18} Surface-sensitive techniques such as sum-frequency generation vibrational spectroscopy and X-ray spectroscopy have been applied to investigate the vapor/liquid interfaces of various ionic liquids.^{19–26} Characterization of surface species as well as molecular orientation can be achieved. However, because the majority of

information of ionic liquids was inferred from experimental measurements, description of most ionic liquids at the molecular level is still incomplete.

Computer simulation techniques provide alternative approaches to study ionic liquid systems.^{26–49} Both molecular dynamics and Monte Carlo methods supply a series of molecular configurations of ionic liquids from which the average molecular structure, thermodynamics, dynamics, as well as intermolecular interactions may be determined. Many theoretical studies have been devoted to the study of the structural and dynamical properties of pure ionic liquids and their interfaces.^{39,43,49–52} Recently, research efforts have also applied to study complex systems that contain an ionic liquid as a component.^{33,40,53–55} These theoretical investigations provide molecular interpretation of the behavior of ionic liquids and contribute greatly to our understanding of them.

It has been long recognized that in order to properly characterize the liquid properties from computer simulation techniques, potential models that adequately describes the molecular interactions are essential. To this end, few groups have attempted to construct and refine force fields for ionic liquids that yield good thermodynamics results.^{36,56,57} Nonetheless, most of these potentials are pairwise additive in nature and do not include the effect of many-body polarization effect. Gray-Weale and Madden have commented that structures of many molten salts may depend sensitively on polarization of their electron clouds and the forces are not pairwise additive in nature.⁵⁸ Recent work by Voth and co-workers investigated the effect of electronic polarizability on the dynamics of ionic liquids. They observed that the effects of polarizability are quite substantial and the polarizable model results are in better agreement with the experimental values than pairwise models for the 1-ethyl-3-methylimidazolium nitrate system.⁵⁹ Bagno and

[†] Part of the “Max Wolfsberg Festschrift”.

* Corresponding author.

co-workers and Picalek and co-workers have recently addressed the significance of the polarization term in the force fields and demonstrated the deficiencies in nonpolarizable simulations for the 1-butyl-3-methylimidazolium tetrafluoroborate ionic liquid.^{60,61} Other groups have also developed new polarizable force fields for ionic liquids and enhanced our understanding of these systems.^{62,63} *Ab initio* molecular dynamics can circumvent the uncertainty associated with potential models by evaluating molecular forces using quantum mechanical methods. However, this method is limited to a small number of ions and short simulation time due to the immense computational requirement associated with electronic structure calculations.^{35,64–67}

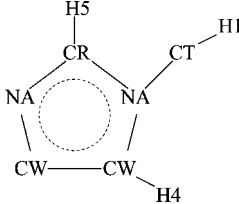
We begin our effort on ionic liquids by constructing all-atom polarizable interaction potential models for one of the most common organic cation of ionic liquids, 1,3-[dmim]⁺ ion. With the new potential model, we will investigate the structural, dynamical, and thermodynamic properties of the bulk and vapor/liquid interface of ionic liquids containing 1,3-dimethylimidazolium cations and three halide anions. In addition, we examine the effect of anion size on the properties of ionic liquids and their interfaces. This paper is organized as follows. The computational details are briefly described in section II. Our simulation results of the bulk ionic liquids and their interfaces including surface tensions and surface potentials are presented and discussed in sections III and IV, respectively. The conclusions are given in section V.

II. Potential Model and Computational Methods

In this study, a many-body polarizable potential model is constructed to describe the interaction of [dmim]⁺ salt melts. The model is based on all-atom framework and includes the effect of induced polarization. The halides, Cl[−], Br[−], and I[−] potential parameters are taken from our early work on ion solvation in aqueous solutions.⁶⁸ The [dmim]⁺ monomer geometry is represented using *ab initio* gas phase values. Fixed charges and Lennard-Jones parameters are assigned to all the atoms of [dmim]⁺. The atomic partial charges are taken from the literature and were extracted from *ab initio* calculations based on electrostatic surface potential fitting.⁵⁰ Atomic polarizabilities are taken from the work of Applequist and co-workers, which were developed using atom-dipole interaction model.⁶⁹ These values are assigned to each atom so that the induction energies and forces can be calculated. The intramolecular potential functions and potential parameters i.e., bond distances, bond angles and dihedral angles are taken from AMBER force fields.^{70,71} The Lennard-Jones parameters of [dmim]⁺ are optimized by carrying out a series of classical molecular dynamics simulations of [dmim]⁺–Cl[−] melts at 423 K. During the parameter optimizations, we calculate the structural and thermodynamic properties of bulk ionic liquids including radial distribution functions and densities and compare to experiments. The final potential parameters are obtained when the potential model adequately reproduces many experimental properties, which are given below, and the parameters are given in Table 1.

MD simulations were performed on bulk solutions of [dmim]⁺ with three different anions, Cl[−], Br[−], and I[−]. All the systems contained 300 ion pairs in a simulation cell of linear dimensions roughly equal to 40 × 40 × 40 Å. Periodic boundary conditions were applied in all three spatial directions. The simulations were carried out in a constant pressure-temperature (NPT) ensemble for structural information and in constant volume-energy (NVE) ensemble for dynamical properties. Since these ionic liquids melt below 400 K,¹⁸ the temperature of the simulations was

TABLE 1: Potential Parameters Used in This Study



atom type	σ (Å)	ϵ (kcal/mol)	q (e)	α (Å ³)
CT	3.296	0.115	−0.1740	0.878
CW	3.332	0.110	−0.1270	0.360
CR	3.332	0.110	−0.1060	0.360
H1	1.960	0.030	0.1310	0.135
H4	2.049	0.026	0.2050	0.167
H5	2.049	0.030	0.2060	0.167
NA	3.136	0.190	0.1530	0.530
Cl ^a	4.339	0.100	−1.0000	3.690
Br ^a	4.543	0.100	−1.0000	4.770
I ^a	5.125	0.100	−1.0000	6.970

^a These potential parameters are taken from ref 68.

maintained at 423 K using the Langevin dynamics thermostat.^{72,73} A time step of 1 fs was used to integrate the equations of motion. The particle mesh Ewald method was employed to handle the long-range Coulombic interactions.^{74,75} During the MD simulations, a standard iterative self-consistent field procedure was used to evaluate the induced dipoles. The iterations were repeated until the deviations of the induced dipoles between two sequential ones fell below a predetermined tolerance value (0.00001 D). All bulk systems were equilibrated for at least 500 ps prior to a 1–2 ns simulation period during which data was collected.

Systems containing 600 ion pairs were also carried out for the air/liquid interface of the three ionic liquids under constant volume-temperature condition. We prepared the liquid/vapor simulation system by taking a pre-equilibrated bulk ionic liquid of linear dimension of 40 × 40 × 80 Å. We then placed it at the center of a supercell with edge lengths 40, 40 and 180 Å thereby forming two vacuum–liquid interfaces with the two free volumes of 50 Å on both sides of z-axis. All of the above-mentioned systems were equilibrated for 3 ns using periodic boundary conditions. The subsequent 3 ns trajectory was then stored at intervals of 1 ps and then used for analysis. We calculated the number densities with respect to the center of mass of the whole systems (i.e., $z = 0$ Å) and thus averaged over the two interfaces.

III. Bulk Melts

A. Thermodynamics. As mentioned earlier, the potential parameters were optimized by fitting the calculated properties to the experimental data of [dmim]⁺–Cl[−] ionic liquids at a temperature of 423 K.^{57,76} The same set of parameters for [dmim]⁺ is then used to determine the properties of [dmim]⁺–Br[−] and [dmim]⁺–I[−] ionic liquids. The computed liquid densities are listed in Table 2. The enthalpy of vaporization of ionic liquids can be evaluated by using the following relation,

$$\Delta H_{\text{vap}} = E_{\text{vap}} - E_{\text{liq}} + RT \quad (1)$$

Here E_{vap} and E_{liq} are the total potential energies in the vapor and liquid phase, respectively. It should be noted that E_{vap} is the potential energy of an isolated ion pair. The results are also listed in Table 2. Clearly, these ionic liquids possess high values of enthalpies of vaporization when compared to ordinary

TABLE 2: Computed Liquid Densities and Enthalpies of Vaporization of the Three Ionic Liquids from MD Simulations at 423 K

system	density (g/cm ³)	ΔH_{vap} (kcal/mol)
[dmim] ⁺ –Cl [–]	1.12 ± 0.05	45.4 ± 0.3
[dmim] ⁺ –Br [–]	1.44 ± 0.06	44.8 ± 0.3
[dmim] ⁺ –I [–]	1.54 ± 0.06	40.7 ± 0.2

molecular solvents. As a consequence, the low volatility makes ionic liquids ideal solvents for chemical processes. The data also clearly demonstrate that the enthalpy of vaporization decreases from Cl[–] to I[–], which can be attributed to decreasing intermolecular interaction with increasing ionic distance.

B. Liquid Structures. The local solvation environment of ionic liquids can be analyzed by their radial distribution functions (RDFs) that are related to the probability of finding other ions at a distance r away from one specific ion. Figure 1a shows the RDF between the cations and anions of the three ionic melts. In these calculations, the center of mass of the imidazolium ring is used to represent the cation. In general, the overall features of these partial RDFs agree reasonably well with the available experimental and computational studies.^{41,43,66,77,78} The well-defined oscillations in the cation–anion partial RDFs clearly indicate that the ionic liquids exhibit long-range, charge-ordered structures. The first peak position of [dmim]⁺–Cl[–] RDF located at a separation of 4.7 Å is consistent with previous works.^{44,65,66,77–79} The RDFs of Cl[–] and Br[–] are similar, while for the larger I[–] anion, the peak position shifts to larger distance and the curve also broadens as expected. All three curves show a well-defined structural correlation at short cation–anion separations due to the strong electrostatic interaction, followed by a much broader second coordination shell.

The cation–cation RDFs are presented in Figure 1b. It is found that the RDFs of all three ionic liquids show a weak first peak at about 4 Å followed by a much broader and more distinct second and third peaks centered at 8 and 14 Å, respectively. The first peak in cation–cation RDFs at short distances can be attributed to the preferential orientational ordering between cations as will be discussed later. The persistent long-range oscillations observed in the RDFs correlates with the view that ionic liquids are strongly ordered systems with solvation structures extending over a longer range than the typical molecular liquids. The cation–cation RDF of [dmim]⁺–Cl[–] ionic liquid is in good agreement with previous work and a recent *ab initio* molecular dynamics study,⁶⁵ but is not consistent with the result derived from the experiment, which has only a small shoulder just below 4 Å and a shallow maximum between 5 and 6 Å.^{77,78} Comparing Figures 1a and 1b, out-of-phase oscillations are clearly found in the cation–anion and cation–cation RDFs. This behavior is due to preferential ionic pairing with alternating layers of cations and anions in the ionic liquid melts. The anion–anion RDFs are shown in Figure 1c. It is clear from Figure 1 that the local structural correlation remains unchanged from Cl[–] to the I[–] anion. The only noticeable difference is that peaks in the RDFs shift to larger distances with increasing anion size, as expected.

C. Dynamics. We begin this section by calculating the normalized translational velocity autocorrelation function, $C_V(t)$, as defined below:

$$C_V(t) = \frac{\langle \vec{V}(t) \cdot \vec{V}(0) \rangle}{\langle \vec{V}(0) \cdot \vec{V}(0) \rangle} \quad (2)$$

Here $\vec{V}(t)$ and $\vec{V}(0)$ are the center-of-mass velocities of ions at time t and time 0, respectively. Displayed in parts a and b of

Figure 2 are the normalized velocity autocorrelation functions of cations and anions in the three ionic liquids, respectively. All curves exhibit features resembled damped oscillations - a fast initial decay to zero (ranging from ~ 0.1 ps for Cl[–] to ~ 0.2 ps for I[–]), followed by some oscillations and eventually reach the asymptotic value of zero. The short-time oscillatory behavior can be explained by the rattling motion of the ion inside the well-organized coordination cage formed by other ions. The negative portion of the autocorrelation function before $C_V(t)$ decays to zero suggests the motion of the ion is hindered. When comparing the three ionic systems, the short-time oscillation is most pronounced in the [dmim]⁺–Cl[–] solution, suggesting that Cl[–] ions experience stronger intermolecular forces. As a result, the coordination shell is more structured and can impede the mobility of ions, leading to a smaller diffusion rate in the [dmim]⁺–Cl[–] melts. Additionally, we found $C_V(t)$ s behave differently in the [dmim]⁺–Cl[–] and [dmim]⁺–Br[–] solutions despite of similar liquid structures (RDFs). This result clearly demonstrates that anion plays an important role in the properties of ionic liquids.

The rotational motion of [dmim]⁺ in these ionic melts was studied via the orientational correlation function, $C_R(t)$

$$C_R(t) = \langle \hat{u}(0) \cdot \hat{u}(t) \rangle \quad (3)$$

where $\hat{u}(t)$ is the body-fixed unit vector along molecular axes of [dmim]⁺ cation at time t . In this study, the three molecular axes are chosen to be the vector connecting the two N atoms in the ring (NN), the molecular C_{2v} symmetry axis, and the surface normal vector of the imidazolium ring. The corresponding orientational correlation functions are shown in Figure 3, parts a–c, respectively. An initial inertial behavior is observed—indicated by the fast decay at short times. After about 2 ps, the autocorrelation functions can be reasonably approximated by single exponential functions (shown as the solid lines in the figure inset) from which the rotational relaxation times can be extracted. The time scales are found to be in the range of 40–120 ps, much longer than those of the velocity autocorrelation functions. Since these correlation functions behave differently, it is evident that the rotation of [dmim]⁺ is anisotropic. The reorientation of the N–N vector occurs at a longer time scale than those of the C_{2v} and surface normal axes in all systems. This result is consistent with the finding of Voth and co-workers on a similar ionic system.⁸⁰ We also note that the identity of the anion is important in the rotational motion of cations, all three axes rotate faster in the ionic liquid containing I[–] anion.

We also calculated the diffusion constants of [dmim]⁺ and I[–]/Br[–]/Cl[–] in these ionic systems from their mean-square displacements (MSD). The data are summarized in Table 3. The computed diffusion rates from present work are slightly higher than those reported by Bhargava et al.^{44,51} and Urahata and co-worker,⁸¹ but are smaller than those reported by Lynden-Bell et al.⁴³ for the same system, but with different force fields. It has been observed that polarizable potential models had the tendency to predict higher diffusion constants in ionic liquids, in agreement with the work here.³⁹ It is also of interest to note that the [dmim]⁺ cation diffuses slightly faster than the anions in all three systems despite of its larger size. This may be due to that the [dmim]⁺ cation can rotate to avoid unfavorable electrostatic interactions between like ions when it moves, while anion motion is hindered by like ions. We also observed anion size influenced the dynamical properties of ions, as the anion size increases from Cl[–] to I[–], both anions and cations move more rapidly.

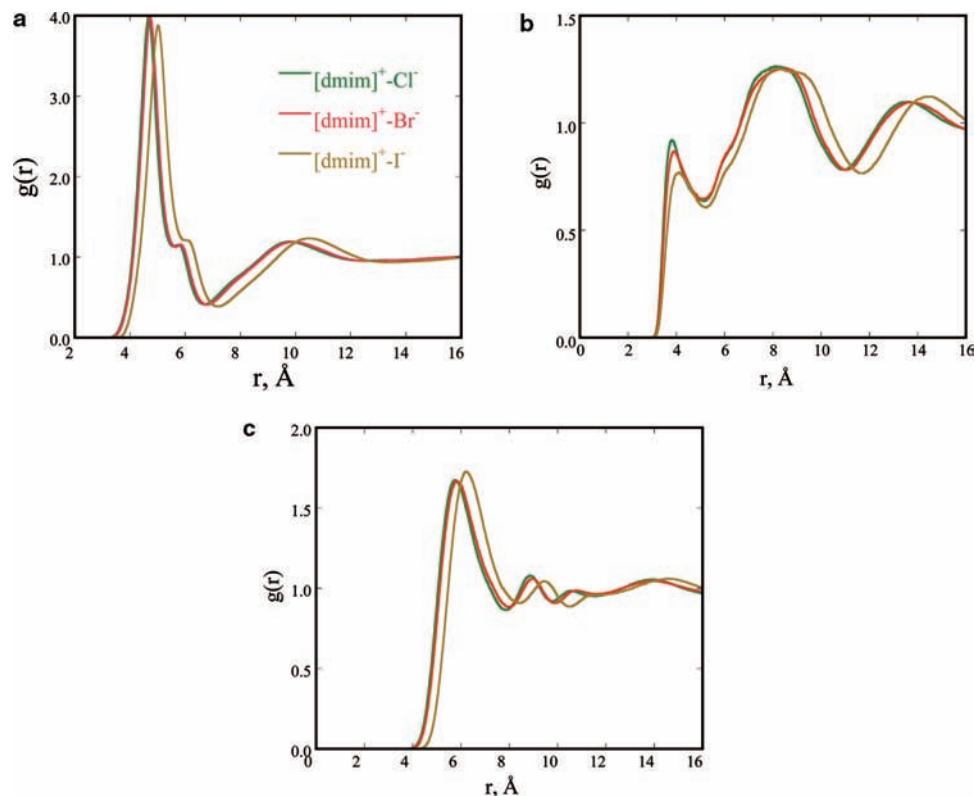


Figure 1. Computed partial radial distribution functions of (a) cation–anion, (b) cation–cation, and (c) anion–anion of 1,3-dimethylimidazolium salt melts. The data points correspond to Cl^- (green), Br^- (red), and I^- (yellow), respectively.

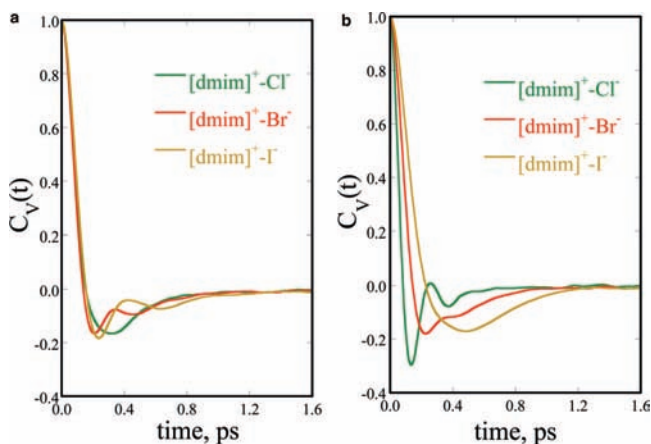


Figure 2. Normalized velocity autocorrelation functions of (a) the center-of-mass of $[\text{dmim}]^+$ cation and (b) the anion at 423 K. The data points correspond to Cl^- (green), Br^- (red), and I^- (yellow), respectively.

We realized that much work has been done on the dynamical properties of the ILs and it has been established that one needs to simulate these systems for a long period (~ 100 ns) in order to observe correct diffusive behavior for a certain ILs (Voth et al.⁸⁰). Although our computed diffusion coefficients over 1.5 ns show only a small difference from early work on the same system (Bhargava and Balasubramanian⁵¹), we realized that the length of the simulations (1.5 ns) is too short and the time range of the MSD data from which the coefficients are calculated could alter the final results. This will be the subject of our future research.

IV. Air/Liquid Interface

Due to the intrinsic inhomogeneous nature of the surface, molecules/ions at the gas/liquid interfaces can be dramatically

modified in their local structures. To understand such interface-induced differences, the number density profile, the structure, and the interfacial thermodynamic properties, such as the surface tension and surface potential, were examined and related to the corresponding experimental measurements.

A. Density Profiles. In Figure 4a, the number density profiles along the interfacial normal direction (z -axis) are plotted for the $[\text{dmim}]^+ - \text{I}^-$ ionic liquid. The three curves correspond to the center-of-mass of the cation, the carbon atom of the methyl group attached to the N atom in the imidazolium ring, and the anion. Few interesting points can be concluded from these graphs. First, the interface is well defined and is relatively sharp on a molecular level. Second, there are noticeable long-range oscillations in the probability profiles. This result was predicted for other ionic liquids and was attributed to the ionic liquids having supercooled liquid-like structures.^{40,82} In particular, the oscillations in the cation and anion density profiles are out-of-phase of each other—when there is an enrichment of cation density, the density of anion is reduced and vice versa, in agreement with the tendency of charge layering observed in ionic liquid melts.^{19,83} We also observe slight enrichment of anion probability near the interface, indicating a tendency for anion to segregate at the interface as demonstrated in Figure 4b. The surface propensity of halide anions at the ionic liquid/vapor interface may be important in their surface reactivity and was predicted by Deutsch et al. from X-ray reflectivity study on similar ionic systems,¹⁹ but it was not found in a previous simulation.³⁰

In addition, we examine the density profiles for various types of atoms of the 1,3-dimethylimidazolium ion. At the top layer of the interface, the probability of finding C atoms of the methyl groups is higher than that of other heavy atoms in the ring, which implies that the methyl groups have a preference to extend into the vapor phase. This behavior has been observed by various

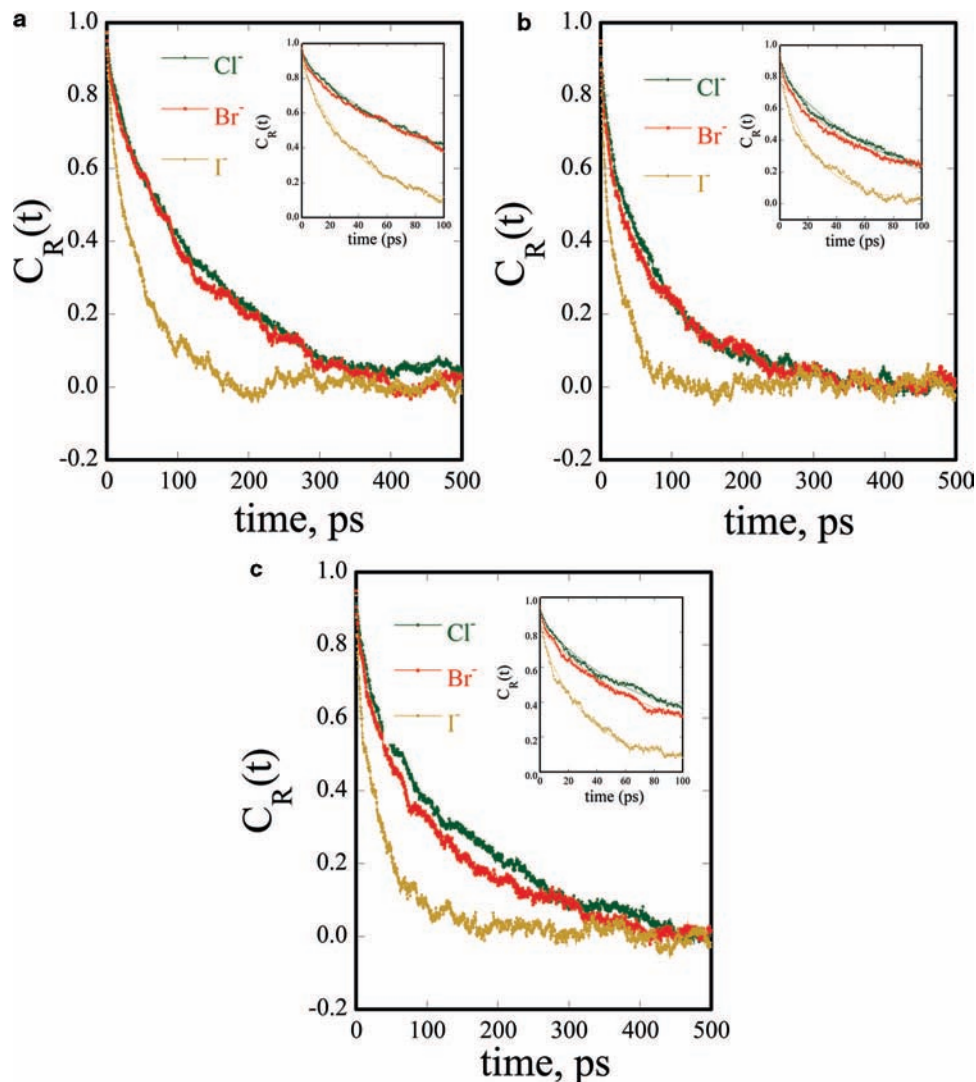


Figure 3. Normalized rotational autocorrelation functions of (a) the NN vector, (b) the C_{2v} molecular axis, and (c) the ring normal of [dmim]⁺ in ionic liquids. The solid curves on the insets indicate the least-squares fits to single exponential function.

TABLE 3: Diffusion Constants (in 10^{-11} m²/s) of Anions and Center-of-Mass of 1,3-Dimethylimidazolium Cation from MD Simulations of Ionic Liquids at 423 K

system	D_{cation}	D_{anion}
[dmim] ⁺ -Cl ⁻	5.7 ± 0.2	4.9 ± 0.2
[dmim] ⁺ -Br ⁻	8.6 ± 0.3	7.2 ± 0.3
[dmim] ⁺ -I ⁻	17.8 ± 0.4	13.6 ± 0.3

experimental techniques^{20–25} including direct recoil spectrometry and angle-resolved X-ray photoelectron spectroscopy for similar ionic liquids.

The change in the local structures of ionic liquid from bulk to the interfacial region can be further examined in terms of the RDFs as a function of the cation z coordinate. In Figure 5, the calculated cation-Cl⁻ and cation-cation RDFs are shown for the [dmim]⁺-Cl⁻ ionic liquid at various cation locations. It is found that the peak locations of these RDFs are independent of their z coordinates. The reduction in the intensity of these RDFs near the interface is simply due to the decreasing number density of cations/anions. This result suggests that the local molecular arrangement of cations and anions remain unchanged from bulk to the interface. However, we found that the intensity of the first peak in the cation-anion RDF remains about the same, indicative of reinforced first coordination shell at the interface due to the strong electrostatic interactions.

B. Surface Tension and Surface Potential. To further evaluate the present interaction model, we calculate the surface tension, γ , which is defined as the difference between the pressure components in the direction parallel and perpendicular to the interface

$$\gamma = \frac{1}{2} \left(\frac{p_{xx} + p_{yy}}{2} - p_{zz} \right) L_z \quad (4)$$

In the above, $p_{\alpha\alpha}$ ($\alpha = x, y, \text{ or } z$) is the $\alpha\alpha$ element of the pressure tensor and L_z is the linear dimension of the simulation cell in the z direction. According to the virial equation, the $\alpha\beta$ element of the pressure tensor is

$$P_{\alpha\beta} = \frac{1}{V} \left(\sum_{i=1}^N m_i v_{i\alpha} v_{i\beta} + \frac{1}{2} \sum_{i'=1}^N \sum_{j'=1}^N F_{i'j'\alpha} r_{i'j'\beta} \right) \quad (5)$$

where N and N' are the numbers of molecules and atoms, respectively. V is the total volume of the system, m_i is the mass of molecule i , and $v_{i\alpha}$ is the center-of-mass velocity of molecule i . In the above expression, $F_{i'j'\alpha}$ is the α component of the force exerted on atom i' of molecule i due to atom j' of molecule j , and $r_{i'j'\beta}$ is the β component of the vector connecting the center of mass of molecules i and j . The calculated surface tensions for the three ionic liquids are 58, 65 and 68 dyn/cm for the [dmim]⁺-I⁻, -Br⁻, and -Cl⁻ systems, respectively, with an

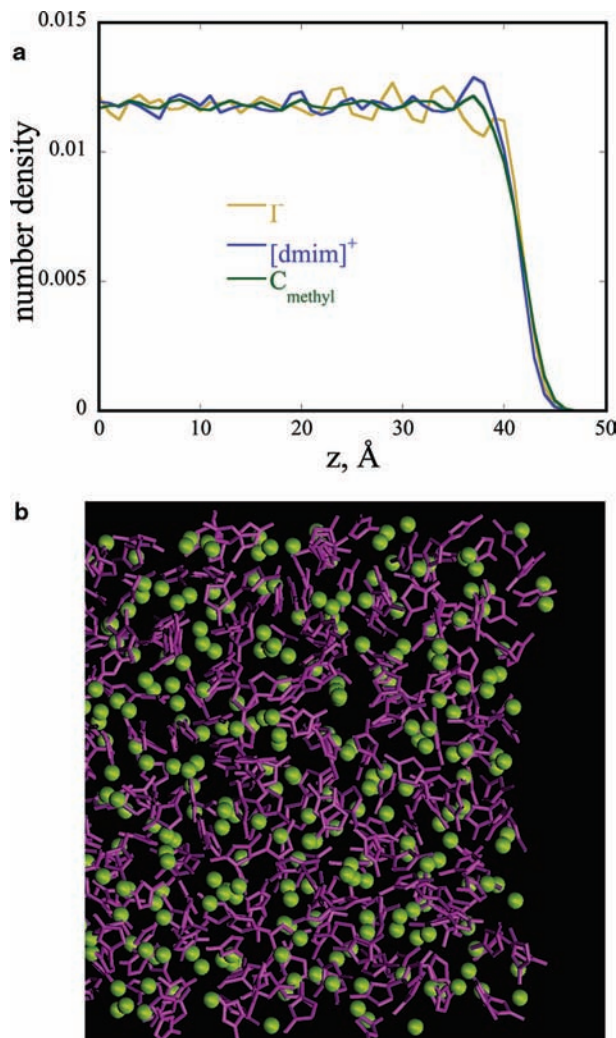


Figure 4. (a) Computed density profiles of the anion (yellow), center-of-mass of the cation (blue), and the methyl C attached to the ring (green) along the interfacial normal direction for the $[dmim]^+I^-$ ionic liquid. (b) Snapshot taken from the MD simulation of the $[dmim]^+I^-$ air/liquid interface.

estimated error bar of ± 5 dyn/cm. In Figure 6, we plot the running average of the surface tensions as a function of simulated time of 3 ns. Our computed surface tensions clearly demonstrated that this property converged extremely slowly up to ~ 2 ns. It is to note that the computed surface tensions of $[dmim]^+Br^-$ and Cl^- are very close together as in the case of their enthalpies of vaporization of bulk ionic liquids.

The surface tensions of various ionic liquids had been measured recently by Law and Watson.⁸⁴ Their results suggest that the surface tension decreases with increasing alkyl chain length for the ionic liquids containing the same anion. For a fixed cation, the ionic system with the larger anion usually has the higher surface tension, but the surface tensions exhibit a narrow range. For instance, the measured surface tensions for the $[omim]^+Br^-$ and Cl^- ionic liquids are 32.0 and 30.5 dyn/cm, respectively. These values are significant smaller than our computed surface tensions due to the longer alkyl chain length, but their difference is quite small and our simulation results show a similar observation. In addition, our computed surface tension for the $[dmim]^+Cl^-$ system is much smaller than the corresponding surface tension reported by Lynden-Bell that employed a nonpolarizable potential model (~ 100 dyn/cm).³⁰ Voith and co-workers have demonstrated recently that the

simulation employed polarizable models gives a surface tension in better agreement with the experimental surface tension and is also smaller than the corresponding value predicted by nonpolarizable model.⁶⁰

The electrostatic potential change across the air-liquid interface was calculated using the atomic approach to determine the effects of the atomic partial charge distributions and induced dipole moments. The electric potential difference across the interface due to the atomic partial charges, $\Delta\phi_q(z)$, is defined as^{85,86}

$$\Delta\phi_q(z) = \phi_q(z) - \phi_q(z_0) = \frac{1}{\epsilon_0} \int_{z_0}^z E_z(z') dz' \quad (6)$$

where z_0 denotes a reference point in the charge-free (air) region and $E_z(z)$ is the electric field derived from point charges as a function of z across the air-liquid interface. $E_z(z)$ is calculated by integrating the charge distribution along the z axis from the air to the liquid phase

$$E_z(z) = \frac{1}{\epsilon_0} \int_{z_0}^z \langle \rho_q(z') \rangle dz' \quad (7)$$

where $\langle \rho_q(z) \rangle$ is the ensemble averaged charge density profile which was evaluated in slabs of 0.25 Å thickness along the z direction. The electrostatic potential due to the induced dipole moment associated with each molecule as a result of its polarizability can be computed as follows

$$\Delta\phi_\mu^{\text{ind}}(z) = \phi_\mu^{\text{ind}}(z) - \phi_\mu^{\text{ind}}(z_0) = \frac{1}{\epsilon_0} \int_{z_0}^z \langle \rho_\mu^{\text{ind}}(z') \rangle dz' \quad (8)$$

The density profile of the induced dipole moments normal to the interface, $\langle \rho_\mu^{\text{ind}}(z) \rangle$, was evaluated as the average of the normal (z) component of the induced dipole moments in the liquid using slabs of 0.25 Å thickness along the z axis. By adding the contributions from the partial charges and induced dipole moments, the total surface potential can be obtained. In essence, a negative surface potential corresponds with a dipoles (either induced or static) pointing toward the interior of the liquid. The data were collected over a 3-ns molecular dynamics simulation after extensive equilibration.

The total electric surface potential as a function of position for all systems studied are given in Figure 7, with the values obtained in the current study for $[dmim]^+I^-$, $[dmim]^+Br^-$ and $[dmim]^+Cl^-$ systems are predicted to be -0.44 ± 0.05 , -0.54 ± 0.05 , and -0.67 ± 0.05 V, respectively. These results clearly demonstrated that the larger anions lead to smaller surface tensions and smaller surface potentials. Upon close examination of Figure 7, we can conclude that the dip in the surface potential near the interface may indicate the presence of a preferred orientational order of $[dmim]^+$ ion and is consistent with the above orientation and local structure analysis. We also observed small oscillations around its averaged values across the interface similar to that of computed number densities. The location of the dip is related to the nature of anions, the larger anion such as the I^- having a dip farther away from the liquid center of mass than the smaller Cl^- . This oscillatory behavior is only observed in the ILs but not in the aqueous interfaces. This fluctuation is the results of the fluctuation in charge density as will be discussed below.

One of the advantages of using polarizable models is that we can evaluate the contributions from the static charges and the induced dipoles to the surface potential. Such evaluation is presented in Figure 8, parts a and b. for the induced dipoles and static charges, respectively. We can make several observations from these results. (1) Because of the polarizable iodide

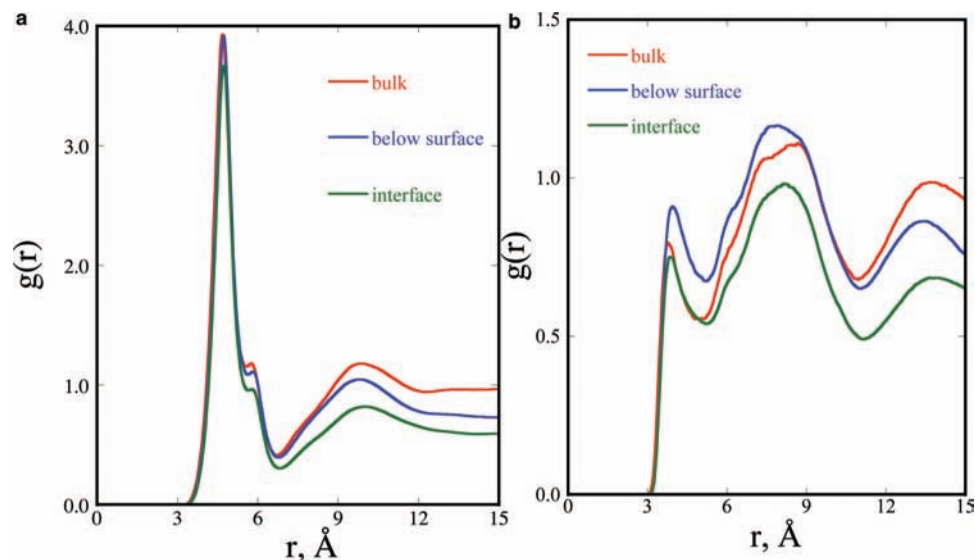


Figure 5. (a) Cation–anion and (b) cation–cation radial distribution function as a function of cation’s location relative to the interface for the $[\text{dmim}]^+\text{-Cl}^-$ ionic solution at 423 K. The three curves correspond to the cations located in the bulk (red), just below the interface (blue), and at the interface (green).

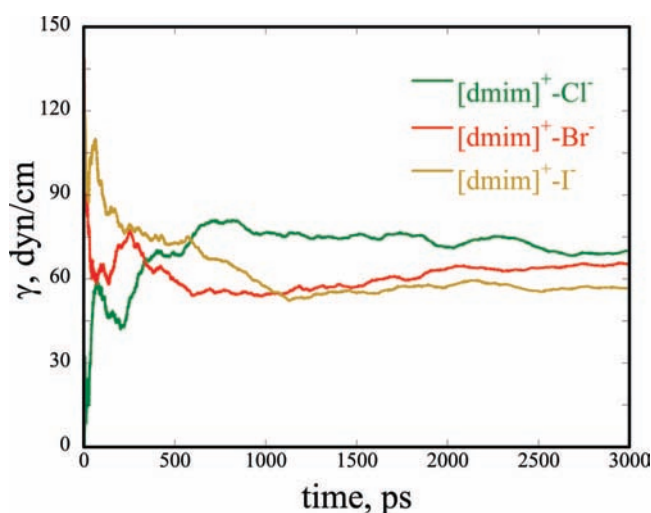


Figure 6. Running average of the surface tension for the interfaces of the three surface ionic $[\text{dmim}]^+\text{-I}^-/\text{-Br}^-/\text{-Cl}^-$ systems.

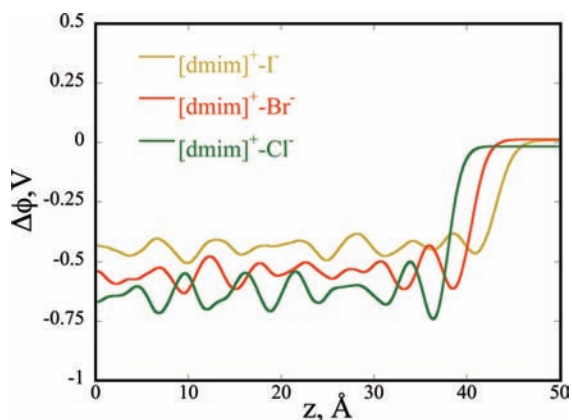


Figure 7. Computed electrostatic surface potentials as a function of z -axis for the $[\text{dmim}]^+\text{-I}^-/\text{-Br}^-/\text{-Cl}^-$ systems.

anion has a largest polarizability, it has the greatest induced dipole contribution (being negative) for the surface potential (see Figure 8a), followed by Br^- and Cl^- . (2) The main contribution to the $[\text{dmim}]^+\text{-Cl}^-$ surface potential is from the static charges, which may be expected since the Cl^- anion is

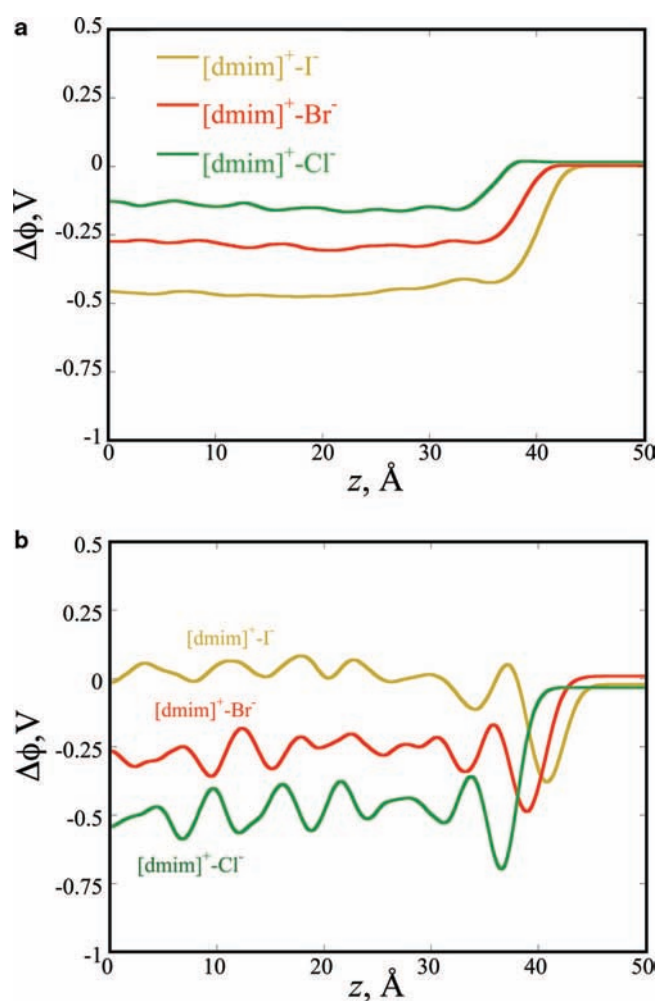


Figure 8. Decomposition of the electrostatic surface potential into the contributions from (a) the induced dipoles (μ) and (b) the static charges (q) for the $[\text{dmim}]^+\text{-I}^-/\text{-Br}^-/\text{-Cl}^-$ systems.

much smaller and the charge–charge interaction in this system is much stronger than the $[\text{dmim}]^+\text{-I}^-$ or -Br^- systems. (3) It is clear that most of the oscillations observed in the computed surface potential are mainly from the fluctuation in the static

charges. This is indicative of surface charge layering at the interface, as observed in the density profiles discussed earlier.

V. Conclusions

Using classical MD simulation techniques, we first constructed an all-atom polarizable potential model to describe the interaction of $[\text{dmim}]^+$. The structural, thermodynamic, and dynamical properties of bulk and liquid/gas interfaces of three ionic liquids, $[\text{dmim}]^+ - \text{Cl}^-$, $[\text{dmim}]^+ - \text{Br}^-$, and $[\text{dmim}]^+ - \text{I}^-$ were investigated. In general, the results are consistent with previous simulations and available experimental data.

In the bulk ionic liquids, it was found that the enthalpies of vaporization were very high in comparison to typical molecular liquids, leading to low volatility, as expected. The calculated partial radial distribution functions exhibit well-defined coordination shells, suggesting there is a strong long-range structural correlation between ions. This is consistent with the concept of charge ordering in the ionic liquids. In these ionic liquids, the anion size does not seem to have significant impact on the static structures.

The single-ion dynamics in these ionic liquids was examined. The ion self-diffusion constants were computed from the mean-square displacements of the center-of-mass of the ions. It was found that the diffusion coefficients are small compared to those of common molecular liquids due to their strong electrostatic interactions. We also found the rotational motion of $[\text{dmim}]^+$ ion is slow and nonisotropic. The reorientation of the N–N vector occurs at a longer time scale than those of C_{2V} and surface normal vectors in three ionic systems. The rotational correlation times were found to be in the range of 40–100 ps, about one magnitude longer than pure water at room temperature. We found the dynamics of ionic liquids was affected by the anions. Both translational and rotational motions of ions are slower in solutions containing Cl^- anions. This behavior can be attributed to the tighter interactions between cations and ions with decreasing size.

The computed density profiles of the ionic liquid/vapor interface showed well-defined interfaces. Noticeable oscillations were observed in these profiles, indicative of surface layering at the interface. There is also a slightly tendency for larger anions to segregate at the interface, which is consistent with recent experimental results. The results of the RDFs provide information of the structures at the interface. It was found that the interface does affect the local molecular environments of the ionic liquids.

The computed surface tensions indicated small differences between these ionic liquids and were found to decrease with the increasing anion size. The surface tension obtained with the polarizable model is also significantly lower than that predicted by the nonpolarizable model, the former being in better agreement with the experimental value. The calculated potential drops of these ionic liquids were found to be small and negative. This result may imply that the cation dipoles are more likely to orient in the interfacial plane than parallel to the surface normal axis.

Our research using MD techniques on ILs can readily be extended into other ILs such as the 1-alkyl-3-methylimidazolium $[\text{amim}]^+ - \text{Cl}^- / -\text{Br}^- / -\text{I}^-$ systems and to other complex molecular processes such as the molecular mechanism of cellulose dissolution in these ILs. The role of water (methanol) at various concentrations in water–(methanol–) ILs mixtures will also be explored to see how they can affect the dynamic and mechanism of molecular processes. Our work using molecular dynamics simulation approaches will provide detailed

molecular-level understanding of the relation between the structure of solvated species and the solvent, the pathway of dissolution of complex molecular systems, and the effect of modifying anions/cations of ILs on these processes.

Acknowledgment. This work was performed at Pacific Northwest National Laboratory (PNNL) under the auspices of the Division of Chemical Sciences, Office of Basic Energy Sciences, U.S. Department of Energy. Battelle operates PNNL for the Department of Energy.

References and Notes

- (1) Wishart, J. F.; Castner, E. W. *J. Phys. Chem. B* **2007**, *111*, 4639.
- (2) Wasserscheid, P. *Nature* **2006**, *439*, 797.
- (3) Welton, T. *Chem. Rev.* **1999**, *99*, 2071.
- (4) Rogers, R. D.; Seddon, K. R. *Science* **2003**, *302*, 792.
- (5) Hermann, W. *Angew. Chem., Int. Ed.* **2008**, *47*, 654.
- (6) Martins, M. A. P.; Frizzo, C. P.; Moreira, D. N.; Zanatta, N.; Bonacorso, H. G. *Chem. Rev.* **2008**, *108*, 2015.
- (7) Dupont, J.; de Souza, R. F.; Suarez, P. A. Z. *Chem. Rev.* **2002**, *102*, 3667.
- (8) Wang, P.; Zakeeruddin, S. M.; Comte, P.; Exnar, I.; Gratzel, M. *J. Am. Chem. Soc.* **2003**, *125*, 1166.
- (9) de Souza, R. F.; Padilha, J. C.; Gonçalves, R. S.; Dupont, J. *Electrochem. Commun.* **2003**, *5*, 728.
- (10) Yoshizawa, M.; Narita, A.; Ohno, H. *Aust. J. Chem.* **2004**, *57*, 139.
- (11) Huddleston, J. G.; Willauer, H. D.; Swatloski, R. P.; Visser, A. E.; Rogers, R. D. *Chem. Commun.* **1998**, 1765.
- (12) Wilkes, J. S.; Levisky, J. A.; Wilson, R. A.; Hussey, C. L. *Inorg. Chem.* **1982**, *21*, 1263.
- (13) Earle, M. J.; Esperanca, J. M. S. S.; Gilea, M. A.; Canongia Lopes, J. N.; Rebelo, L. P. N.; Magee, J. W.; Seddon, K. R.; Widegren, J. A. *Nature* **2006**, *439*, 831.
- (14) Noda, A.; Hayamizu, K.; Watanabe, M. *J. Phys. Chem. B* **2001**, *105*, 4603.
- (15) Dupont, J.; Suarez, P. A. Z. *Phys. Chem. Chem. Phys.* **2006**, *8*, 2441.
- (16) Iwata, K.; Okajima, H.; Saha, S.; Hamaguchi, H. O. *Acc. Chem. Res.* **2007**, *40*, 1174.
- (17) Castner, E. W.; Wishart, J. F.; Shirota, H. *Acc. Chem. Res.* **2007**, *40*, 1217.
- (18) Zhang, S. J.; Sun, N.; He, X. Z.; Lu, X. M.; Zhang, X. P. *J. Phys. Chem. Ref. Data* **2006**, *35*, 1475.
- (19) Solutskin, E.; Ocko, B. M.; Taman, L.; Kuzmenko, I.; Gog, T.; Deutsch, M. *J. Am. Chem. Soc.* **2005**, *127*, 7796.
- (20) Bowers, J.; Vergara-Gutierrez, M. C.; Webster, J. R. P. *Langmuir* **2004**, *20*, 309.
- (21) Gannon, T. J.; Law, G.; Watson, P. R.; Carmichael, A. J.; Seddon, K. R. *Langmuir* **1999**, *15*, 8429.
- (22) Lockett, V.; Sedev, R.; Bassell, C.; Ralston, J. *Phys. Chem. Chem. Phys.* **2008**, *10*, 1330.
- (23) Law, G.; Watson, P. R.; Carmichael, A. J.; Seddon, K. R.; Seddon, B. *Phys. Chem. Chem. Phys.* **2001**, *3*, 2879.
- (24) Santos, C. S.; Rivera-Rubero, S.; Dibrov, S.; Baldelli, S. *J. Phys. Chem. C* **2007**, *111*, 7682.
- (25) Iimori, T.; Iwahashi, T.; Ishii, H.; Seki, K.; Ouchi, Y.; Ozawa, R.; Hamaguchi, H.; Kim, D. *Chem. Phys. Lett.* **2004**, *389*, 321.
- (26) Rivera-Rubero, S.; Baldelli, S. *J. Phys. Chem. B* **2006**, *110*, 4756.
- (27) Schroder, C.; Steinhäuser, O. *J. Chem. Phys.* **2008**, *128*, 224503.
- (28) Raabe, G.; Koehler, J. *J. Chem. Phys.* **2008**, 128.
- (29) Padua, A. A. H.; Gomes, M. F.; Lopes, J. *Acc. Chem. Res.* **2007**, *40*, 1087.
- (30) Lynden-Bell, R. M. *Mol. Phys.* **2003**, *101*, 2625.
- (31) Lynden-Bell, R. M.; Del Popolo, M. G.; Youngs, T. G. A.; Kohanoff, J.; Hanke, C. G.; Harper, J. B.; Pinilla, C. C. *Acc. Chem. Res.* **2007**, *40*, 1138.
- (32) Sieffert, N.; Wipff, G. *J. Phys. Chem. B* **2007**, *111*, 7253.
- (33) Sieffert, N.; Wipff, G. *J. Phys. Chem. B* **2007**, *111*, 4951.
- (34) Bagno, A.; D'Amico, F.; Saielli, G. *J. Phys. Chem. B* **2006**, *110*, 23004.
- (35) Ghatee, M. H.; Ansari, Y. *J. Chem. Phys.* **2007**, *126*, 154502.
- (36) Lopes, J. N. C.; Padua, A. A. H. *J. Phys. Chem. B* **2006**, *110*, 19586.
- (37) Prado, C. E. R.; Del Popolo, M. G.; Youngs, T. G. A.; Kohanoff, J.; Lynden-Bell, R. M. *Mol. Phys.* **2006**, *104*, 2477.
- (38) Hunt, P. A. *Mol. Simul.* **2006**, *32*, 1.
- (39) Yan, T. Y.; Burnham, C. J.; Del Popolo, M. G.; Voth, G. A. *J. Phys. Chem. B* **2004**, *108*, 11877.
- (40) Yan, T. Y.; Li, S.; Jiang, W.; Gao, X. P.; Xiang, B.; Voth, G. A. *J. Phys. Chem. B* **2006**, *110*, 1800.

- (41) Urahata, S. M.; Ribeiro, M. C. C. *J. Chem. Phys.* **2004**, *120*, 1855.
(42) Hanke, C. G.; Lynden-Bell, R. M. *J. Phys. Chem. B* **2003**, *107*, 10873.
(43) Hanke, C. G.; Price, S. L.; Lynden-Bell, R. M. *Mol. Phys.* **2001**, *99*, 801.
(44) Bhargava, B. L.; Balasubramanian, S. *J. Chem. Phys.* **2005**, *123*, 144505.
(45) Anthony, J. L.; Maginn, E. J.; Brennecke, J. F. *J. Phys. Chem. B* **2002**, *106*, 7315.
(46) Morrow, T. I.; Maginn, E. J. *J. Phys. Chem. B* **2002**, *106*, 12807.
(47) Maginn, E. J. *Acc. Chem. Res.* **2007**, *40*, 1200.
(48) Cadena, C.; Anthony, J. L.; Shah, J. K.; Morrow, T. I.; Brennecke, J. F.; Maginn, E. J. *J. Am. Chem. Soc.* **2004**, *126*, 5300.
(49) Margulis, C. J.; Stern, H. A.; Berne, B. J. *J. Phys. Chem. B* **2002**, *106*, 12017.
(50) Lopes, J. N. C.; Deschamps, J.; Padua, A. A. H. *J. Phys. Chem. B* **2004**, *108*, 2038.
(51) Bhargava, B. L.; Balasubramanian, S. *J. Chem. Phys.* **2006**, *125*, 219901.
(52) Lee, S. U.; Jung, J.; Han, Y.-K. *Chem. Phys. Lett.* **2005**, *406*, 332.
(53) Kelkar, M. S.; Maginn, E. J. *J. Phys. Chem. B* **2007**, *111*, 4867.
(54) Bhargava, B. L.; Balasubramanian, S. *J. Phys. Chem. B* **2007**, *111*, 4477.
(55) Wu, X. P.; Liu, Z. P.; Huang, S. P.; Wang, W. C. *Phys. Chem. Chem. Phys.* **2005**, *7*, 2771.
(56) de Andrade, J.; Boes, E. S.; Stassen, H. *J. Phys. Chem. B* **2002**, *106*, 3546.
(57) Liu, Z. P.; Huang, S. P.; Wang, W. C. *J. Phys. Chem. B* **2004**, *108*, 12978.
(58) Gray-Weale, A.; Madden, P. A. *Mol. Phys.* **2003**, *101*, 1761.
(59) Wang, Y.; Jiang, W.; Yan, T.; Voth, G. A. *Acc. Chem. Res.* **2007**, *40*, 1193.
(60) Bagnò, A.; D'Amico, F.; Saielli, G. *J. Mol. Liq.* **2007**, *131*, 17.
(61) Picalek, J.; Minofar, B.; Kolafa, J.; Jungwirth, P. *Phys. Chem. Chem. Phys.* **2008**, *10*, 5765.
(62) Hu, Z. H.; Huang, X. H.; Annapureddy, H. V. R.; Margulis, C. J. *J. Phys. Chem. B* **2008**, *112*, 7837.
(63) Smith, G. D.; Borodin, O.; Li, L.; Kim, H.; Liu, Q.; Bara, J. E.; Gin, D. L.; Nobel, R. *Phys. Chem. Chem. Phys.* **2008**, *10*, 6301.
(64) Del Popolo, M. G.; Lynden-Bell, R. M.; Kohanoff, J. *J. Phys. Chem. B* **2005**, *109*, 5895.
(65) Buhl, M.; Chaumont, A.; Schurhammer, R.; Wipff, G. *J. Phys. Chem. B* **2005**, *109*, 18591.
(66) Bhargava, B. L.; Balasubramanian, S. *Chem. Phys. Lett.* **2006**, *417*, 486.
(67) Bagnò, A.; D'Amico, F.; Saielli, G. *Chem. Phys. Chem.* **2007**, *8*, 873.
(68) Dang, L. X. *J. Phys. Chem. B* **2002**, *106*, 10388.
(69) Applequist, J.; Carl, J. R.; Fung, K.-K. *J. Am. Chem. Soc.* **1972**, *94*, 2952.
(70) Cornell, W. D.; Cieplak, P.; Bayly, C. I.; Gould, I. R.; Merz, K. M.; Ferguson, D. M.; Spellmeyer, D. C.; Fox, T.; Caldwell, J. W.; Kollman, P. A. *J. Am. Chem. Soc.* **1995**, *117*, 5179.
(71) de Andrade, J.; Boes, E. S.; Stassen, H. *J. Phys. Chem. B* **2002**, *106*, 13344.
(72) Pastor, R. W.; Brooks, B. R.; Szabo, A. *Mol. Phys.* **1988**, *65*, 1409.
(73) Izaguirre, J. A.; Catarello, D. P.; Wozniak, J. M.; Skeel, R. D. *J. Chem. Phys.* **2001**, *114*, 2090.
(74) Darden, T.; York, D.; Pedersen, L. *J. Chem. Phys.* **1993**, *98*, 10089.
(75) Essmann, U.; Perera, L.; Berkowitz, M. L.; Darden, T.; Lee, H.; Pedersen, L. G. *J. Chem. Phys.* **1995**, *103*, 8577.
(76) Fannin, A. A. J.; Floreani, D. A.; King, L. A. *J. Phys. Chem.* **1984**, *88*, 2614.
(77) Hardacre, C.; Holbrey, J. D.; McMath, S. E. J.; Bowron, D. T.; Soper, A. K. *J. Chem. Phys.* **2003**, *118*, 273.
(78) Hardacre, C.; McMath, S. E. J.; Nieuwenhuysen, M.; Bowron, D. T.; Soper, A. K. *J. Phys.: Condens. Matter* **2003**, *15*, S159.
(79) Qiao, B.; Krekeler, C.; Berger, R.; Delle Site, L.; Holm, C. *J. Phys. Chem. B* **2008**, *112*, 1743.
(80) Del Popolo, M. G.; Voth, G. A. *J. Phys. Chem. B* **2004**, *108*, 1744.
(81) Urahata, S. M.; Ribeiro, M. C. C. *J. Chem. Phys.* **2005**, *122*, 024511.
(82) Jiang, W.; Wang, Y. T.; Yan, T. Y.; Voth, G. A. *J. Phys. Chem. C* **2008**, *112*, 1132.
(83) Bhargava, B. L.; Balasubramanian, S. *J. Am. Chem. Soc.* **2006**, *128*, 10073.
(84) Law, G.; Watson, P. R. *Chem. Phys. Lett.* **2001**, *345*, 1.
(85) Paluch, M. *Adv. Colloid Interface Sci.* **2000**, *84*, 27.
(86) Sokhan, V.; Tildesley, D. J. *Mol. Phys.* **1997**, *92*, 625.